Ω

SPE 30541

Steady-State Relative Permeability Measurements Corrected for Capillary Effects

G.A. Virnovsky, SPE, Rogaland Research, S.M. Skjæveland, SPE, Rogaland University Centre, J. Surdal, Statoil, P. Ingsøy, SPE, Esso Norge

Abstract

A new method is presented which enables to interpret steady-state flow experiments eliminating errors caused by the capillary end-effect. This is achieved by retaining the capillary term in the equations that are used to interpret the flow data.

The standard experimental procedure has to be extended to include variations in both total flowrate and the ratio of phase flowrates. Consistent values of saturation and relative permeability of each phase are then calculated at the inlet end.

Necessary modifications in laboratory procedures and influence of hysteresis are discussed and the theoretical development is exemplified by numerical simulation of coreflood experiments.

Introduction

During a steady-state procedure for measurement of relative permeability curves, the total flowrate of oil and water is usually kept constant while their ratio is changed at the inlet end of the core. After a change, it is necessary to wait until equilibrium in the core is re-established, i.e., when both the pressure drop and the effluent flowrate ratio do not change with time. The individual flowrates and the pressure drop is then used to calculate the individual phase relative permeability values by Darcy's law, relating them to the average saturation in the core, determined by material balance.

The main inaccuracies of this method stem from the basic assumption that the capillary pressure can be neglected[11,13]. Actually, because of capillary effects, the saturation distribution along the core is non-uniform, and the pressure drop is different in each phase. The capillary effects are difficult to avoid even if the total flowrate is high and for some rocks high flowrate cannot be reached for reasons like limited equipment capacity or stress that may cause rock damage.

In this paper a new steady-state technique is described that includes capillary effects.

The proposed experimental setup is not very much different from that of the conventional steady-state method. For a fixed fractional flow at the inlet, a number of steady-state experiments is required with varying total flowrate to include the capillary effect in the analysis of the data. The capillary pressure curve has to be measured separately.

Theory

The following standard equations describe one-dimensional, two-phase flow of immiscible, incompressible fluids in a porous medium[7],

$$u_i = -k\lambda_i \frac{\partial p_i}{\partial x}, \quad i = 1,2$$

$$u_t = -k\lambda_t \frac{\partial p_1}{\partial x} - k\lambda_2 \frac{\partial p_c}{\partial x}, \tag{1}$$

$$p_c(S) = p_2 - p_1.$$

From Eqs. (1) it follows that the expression for the velocity of the first phase is

$$u_1 = u_t f + kf\lambda_2 \frac{\partial p_c}{\partial x}. \tag{2}$$

Conservation of mass gives

$$\frac{\partial u_1}{\partial x} + \phi \frac{\partial S_1}{\partial t} = 0. \tag{3}$$

Let us consider steady-state flow only. Then the saturation in the core is solely a function of the x-coordinate. Since

$\partial S_1 / \partial t = 0$, integration of (3) then shows that the expression

$$u_1 = u_t F \tag{4}$$

is a constant. Here $F = u_1 / u_t$ denotes the fixed fractional flow at the inlet. From Eqs. (2) and (4) it follows that

$$u_t(f - F) + kf\lambda_2 \frac{d p_c}{dx} = 0, \tag{5}$$

$$\frac{\Delta p_1 k}{u_t F} = \int_0^L \frac{dx}{\lambda_1}, \quad \Delta p_1 = p_1(0) - p_1(L),$$

$$dx = kf\lambda_2 \frac{dp_c}{u_t(F - f)},$$

$$\frac{\Delta p_1 k}{u_t F} = \int_0^L \frac{1}{\lambda_1} kf\lambda_2 \frac{dp_c}{u_t(F - f)},$$

$$= \frac{k}{u_t} \int_{p_c^0}^{p_c^L} \frac{(1 - f)dp_c}{(F - f)},$$

where

$$p_c^0 = p_c\big|_{x=0}, \qquad p_c^L = p_c\big|_{x=L}.$$

The expressions for phase pressure drops across the core are then

$$\Delta p_1 = F \int_{p_c^0}^{p_c^L} \frac{(1 - f)dp_c}{(F - f)}, \tag{6a}$$

and

$$\Delta p_2 = (1 - F) \int_{p_c^0}^{p_c^L} \frac{f dp_c}{(F - f)}. \tag{6b}$$

The total velocity follows from Eq. (5) by integration,

$$u_t = -\frac{k}{L} \int_{p_c^0}^{p_c^L} \frac{f\lambda_2 dp_c}{(f - F)}, \tag{7}$$

and the average saturation is

$$\bar{S}(F) = \frac{k}{u_t L} \int_{p_c^0}^{p_c^L} S \frac{f\lambda_2}{(F - f)} dp_c, \tag{8}$$

with

$$\bar{S} = \frac{1}{L} \int_0^L S(x)dx.$$

Eqs. (6), (7), and (8) relate the measurable quantities, i.e., pressure drop in each of the phases, total velocity, and average saturation in the core, to the unknown functions f, λ_2, and S. The last two equations have been considered in Ref. [10] for the particular case when $F = 0$ to develop a method for the interpretation of steady-state experiments.

The two main control parameters of the method are F and u_t. Let us consider the case when F is constant while u_t is varied. As explained below, the capillary pressure at the outlet of the core is constant. Hence, by differentiation of Eqs. (6)–(8) with respect to capillary pressure at the inlet end, p_c^0, one obtains

$$\frac{d\Delta p_1}{dp_c^0} = -\frac{F(1 - f)}{(F - f)}, \tag{9a}$$

$$\frac{d\Delta p_2}{dp_c^0} = -\frac{(1 - F)f}{(F - f)}, \tag{9b}$$

$$\frac{du_t}{dp_c^0} = \frac{k}{L} \frac{f\lambda_2}{(f - F)}, \tag{10}$$

$$\frac{d(\bar{S}u_t)}{dp_c^0} = -\frac{k}{L} S \frac{f\lambda_2}{(F - f)}. \tag{11}$$

From (10) and (11) it follows that

$$\frac{d(\bar{S}u_t)}{du_t} = S(x = 0), \tag{12}$$

and from (9) and (10) that

$$\frac{d\Delta p_1}{du_t} = \frac{F}{\lambda_1} \frac{L}{k}, \quad \frac{d\Delta p_2}{du_t} = \frac{(1 - F)L}{k\lambda_2}, \tag{13a}$$

$$\lambda_1 = \frac{F}{\frac{d\Delta p_1}{du_t}} \frac{L}{k}, \qquad \lambda_2 = \frac{(1 - F)}{\frac{d\Delta p_2}{du_t}} \frac{L}{k}. \tag{13b}$$

All the saturation-dependent quantities in Eqs. (13) are referred to the saturation at the inlet end, as determined by Eq. (12).

A number of possibilities to apply the formulae (12) and (13) is possible depending on what input information is available, i.e., whether the individual phase pressure drops are measured, and whether the capillary pressure is measured separately[14].

We further assume that the capillary pressure curve is measured separately. Then, if individual pressure drop across the core corresponding to one of the flowing phases is measured, the other one can be easily calculated since the saturation at inlet is calculated from Eq. (12) independently of pressures (it depends only on measured volumes).

Corrections for Capillary Effects

Let us denote

$$\tilde{k}_{ri} = \frac{u_i L \mu_i}{\Delta p_i k} = \frac{u_t F_i L \mu_i}{\Delta p_i k}, \qquad i = 1,2 \tag{14}$$

Then, after substitution of Eqs. (14) into Eqs. (13b) and some algebra, the following expressions are easily obtained:

$$k_{ri}(S^0) = \tilde{k}_{ri}\left[1 - \frac{u_t}{\tilde{k}_{ri}}\frac{d\tilde{k}_{ri}}{du_t}\right]^{-1}, \qquad i = 1,2 \tag{15}$$

The formula is exact. Assuming the second term in the brackets to be small as compared to unity, we have an approximate expression

$$k_{ri}(S^0) = \tilde{k}_{ri} + u_t \frac{d\tilde{k}_{ri}}{du_t}, \tag{16}$$

Correction of the saturation:
From eq. (12) we have

$$S^0 = \frac{d(\bar{S}u_t)}{du_t} = \bar{S} + u_t \frac{d\bar{S}}{du_t}, \tag{17}$$

Boundary Conditions

Several practical difficulties may be envisioned when trying to apply the method. One of the main obstacles is how to measure the phase pressures. Ramakrishnan and Capiello[10] suggested to inject only the nonwetting phase at different rates in a core initially saturated with the wetting phase. Then $F = 0$ in Eqs. (13). The disadvantage is obvious: the relative permeability of the wetting phase cannot be determined. Also, only drainage curves can be measured.

The phase pressures may in principle be monitored in the porous medium itself by the technique of semipermeable pads[11]. However, the method is complicated and expensive and probably not viable for routine measurements.

Another method is to measure the phase pressures outside the core, in the tubing or grooves of the endpiece, provided that each phase pressure is continuous from the endpiece and into the core.

Pressure Traverses

Behavior of phase pressures across the core boundaries has been extensively discussed theoretically[2,7,12,16]. A numerical study is reported in Ref. [15]

Outlet End. The capillary pressure outside the core in the receiving end piece is assumed to be equal to zero.

If the flow process in the core is drainage and the capillary pressure curve is non zero and positive for all saturation values, e.g., a water-wet system, pressure continuity at the outlet cannot be satisfied for both phases[2,12]. The saturation of the nonwetting phase at the core outlet corresponds to the lowest possible capillary pressure inside the core and the relative permeability of the nonwetting phase is close to zero. As explained in Ref. [2], the nonwetting phase pressure is discontinuous and the wetting phase pressure is continuous. This is in agreement with the experiments of Richardson *et. al*[11] who state that the magnitude of the discontinuity is equal to the capillary pressure at the equilibrium nonwetting fluid saturation.

For an imbibition process, however, the capillary pressure curve is zero for some saturation, i.e., the endpoint of an spontaneous imbibition process. The outlet end saturation is fixed at this value, both phase pressures are continuous and the capillary pressure is zero and continuous across the boundary.

Experimentally, for a drainage process, a slight fluctuation in injection pressure, say, may shift the flow process at the outlet from drainage to imbibition, resulting in zero capillary pressure and continuity of both phases at the outlet.

Consequently, the capillary pressure at the outlet boundary of the core only depends on the properties of the relevant capillary pressure curve. It remains constant at different flowrates and may be zero or not, depending on the wettability of the core and type of displacement process.

Inlet End. With the saturation at the outlet boundary given as discussed above, the steady state saturation distribution in the core is defined by Eq. (5), so that the saturation in the core close to the inlet boundary, S_i^+ and the corresponding capillary pressure $p_c^+(S_i^+)$, may uniquely be determined.

If the two phase pressures are equal on the outside of the inlet end, there will be a discontinuity of the wetting phase pressure going into the core, provided $p_c^+(S_i^+)$ is nonzero. Otherwise, there would have been backflow of the nonwetting phase, contrary to the imposed boundary conditions of constant rate injection. However, if the two phases are injected into the core at different pressures through wetting and nonwetting membranes, both phase pressures will be continuous.

Pressure Drop Across the Core. Since the nonwetting phase pressure is continuous at the inlet and the capillary pressure is constant at the outlet, it follows that the total pressure drop measured outside porous medium corresponds to the pressure drop in the nonwetting phase plus a constant value equal to the capillary pressure at the outlet.

For an imbibition process, both phase pressures are continuous at the outlet end since the capillary pressure there is zero. At the inlet boundary, the wetting phase pressure is discontinuous. In this case, therefore, the pressure drop measured outside the core is equal to the pressure drop of the nonwetting phase through the core.

With the existing laboratory equipment, only the pressure drop outside the core is measurable in practice. An attempt to measure the individual phase pressure drops over the porous medium will generally give large errors because of the pressure discontinuities across the boundaries of the porous medium.

In this situation, only the phase mobility of the nonwetting phase may be determined if the capillary pressure curve is unknown *a priori*. If the capillary pressure curve is known, then the individual wetting phase pressure and the wetting phase relative permeability may be determined.

Examples

A number of numerical experiments has been performed to test the interpretation procedure according to the following scheme: (1) simulate a multirate, steady-state experiment by a numerical coreflood simulator; (2) use the artificial data with or without addition of random errors to back-calculate the (input) relative permeability and capillary pressures curves.

Simulation Grid. A total of 72 blocks was used in the one-dimensional simulations. The first numerical block is the injection block with high k and low ϕ. The pressure drop of the phases across the core is represented by the difference in pressure between the first core block (second numerical block) and the core outlet. Some grid refinement is used at the core inlet and outlet ends. The block lengths are for Δx(1-72): 2*0.01, 4*0.02, 3*0.1, 40*0.4, 15*0.2, 5*0.1, 2*0.05.

Core and Fluid Data. L = 20.0 cm; A = 10.64 cm^2; ϕ = 22%; $k_o(S_{iw})$ = 485 mD; k_r: Corey type with exponents equal to 2.0; $k_{ro}(S_{iw}) = k_{rw}(S_{or})$ = 1.0; μ_o = 1.06 cp; μ_w = 1.30 cp.

Two capillary pressure curves were used; a p_c-curve for a typical water-wet core, and one for a mixed-wet core. Hysteresis effects are not included.

Simulation of Multirate Steady-Steady Floods. Generally, starting at irreducible water saturation, oil and water are injected with stepwise constant rates according to a preset schedule of fractional flow values and total injection rates. For the examples presented here, the fractional flow is stepwise held constant while the total rate is increased in 20 steps. The rate-change schedule should be chosen such that the water saturation strictly increases at all positions along the core to avoid a mixture of hysteresis effects and subsequent difficulties with the interpretation. This implies that the rate-change schedule should be designed dependent on the wettability of the core sample.

For the water-wet case, Fig. 1 shows the fractional flow values (3), the rate schedule, the average water saturation, and the oil and water pressures at the inlet end. Fig. 2 gives the corresponding saturation profiles. Note that the water saturation profiles reveal a nonmonotonous development with possible mixed hysteresis effects. The experimental procedure must therefore be studied more in detail to find general guidelines to avoid this effect.

The corresponding data for the mixed-wet case are displayed in Figs. 3 and 4, now with 2 injection ratios.

Interpretation

Water-Wet Core. Only a portion of data which corresponds to F_w=*0.01* (see Figs. 1,2) is used. The calculated relative permeabilities of oil and water shown by filled and open circles in Fig. 5 are very close to the true values (simulator input) represented by solid lines. Also shown are the relative permeabilities of oil (filled squares) and water (open squares) calculated from Darcy's law, i.e., without account for capillary effects. One may observe large errors caused by the negligence of capillarity even for relatively large total rates corresponding to low water saturations.

If capillary effects are not properly accounted for, the interpretation errors become especially large for the wetting phase because of the error in pressure drop. As discussed above, the pressure drop measured in the tubing outside porous medium is for the nonwetting phase if the capillary pressure at the outlet is zero, as it is in this example. The relative error in the wetting phase pressure drop increases when the total rate decreases because of increasing dominance of capillary forces.

The sensitivity of the interpretation algorithm to measurement errors has been tested. Pressure drops and phase volumes were subjected to a 1% random error level and two smoothening intervals were tested. The results, not shown here, were quite satisfactory for both capillary pressure and relative permeabilities. The 1% error level, which may be regarded as realistic, leads to errors in the calculated relative permeabilities which is lower than the errors resulting from neglect of capillary effects even without measurement errors.

The Nsm-label in the figures is half the number of measurement points included in the smoothening interval.

Mixed-Wet Core. The simulated results for the two fractional flow values of 1% and 99% of water are shown in Figs. 3 and 4. The calculated and the true relative permeabilities are presented in Fig. 6 for the case of no errors introduced. The saturation interval is fairly well covered by just the two fractional flow values used.

When errors are artificially introduced, the results are qualitatively the same as for the water-wet core discussed above.

Note that for all rates and fractional flow values the saturation at the outlet end in Fig. 4 remains fixed at 0.5, the value where the input capillary pressure curve is zero. Both phase pressures are therefore continuous at the outlet end for this case.

Hysteresis

From simulated saturation profiles (saturation versus length) presented in Fig. 2, it is observed that hysteresis may occur when the water fraction and the total rate are varied independently. For a water wet core, the sequence of saturation profiles for decreasing values of u_t at a fixed F_W = 0.01 may overlap with the saturation profiles for decreasing u_t at fixed F_W = 0.50, especially in the downstream half of the core.

To implement hysteresis in a numerical reservoir simulator, Killough[5] suggested a mathematical model that has gained wide popularity[4,8,9]. The relative permeability and capillary pressure values are enveloped by boundary curves, i.e., primary drainage and imbibition. Transitional scanning curves between the boundary curves are formulated by equations with a couple of additional parameters. Other mathematical models[5] use transformations of the boundary curves to represent the scanning curves.

The Killough model does not allow for separate specification of the secondary drainage curve. It is treated as a scanning curve between primary drainage and imbibition. During many reservoir flow processes, however, e.g., water and gas coning, hysteresis will take place between the imbibition and secondary drainage curves. The secondary drainage curve is actually a boundary curve for the scanning curves and may be quite different from the primary drainage curve, at least for the nonwetting case[1]. Also, the secondary drainage curve for the relative permeability of the nonwetting phase may be lower than the imbibition curve, as measured by Braun and Holland[1].

For the simulations of laboratory experiments presented in this paper, we have used a commercial simulator[4] with the Killough option. The relative permeability and capillary pressure curves for primary drainage and imbibition were input and the secondary drainage curve was constructed by the simulator as a scanning curve.

Steady-state experiments on a core with standard properties and fluids (oil and water) were simulated by the use of a one-dimensional grid with 562 numerical blocks with some refinement at the ends. The blocks at each end were given zero capillary pressure.

Different sequences of drainage and imbibition processes were simulated and checked for hysteresis by plotting the saturation profiles and looking for overlap. The following sequence of (u_t, F_W)-values may be used to avoid hysteresis while measuring the boundary curves (primary drainage, imbibition, secondary drainage) of both relative permeabilities and capillary pressure for a waterwet core.

1. Start with the core 100% saturated with water, or as high water saturation as possible, i.e., at S_{orw} for fresh cores.

2. Primary drainage starts at F_W = 1 and is reduced in steps of 0.1 and terminated at F_W = 0. At each new level, the total rate u_t is increased in one or two small steps to estimate the derivatives with respect to u_t at constant F_W from Eqs. (15), (17) For a fresh core, starting at S_{orw}, this drainage would give the secondary drainage boundary curve.

3. Uniform, irreducible water saturation is then established by for instance the use of a waterwet and an oilwet membrane at the outlet and inlet ends, respectively[6].

4. Imbibition is performed by increasing the levels of F_W from 0 and the total rate is decreased by a small step at each new level.

5. The secondary drainage process is performed as for the primary drainage case.

The main point is, of course, that the changes in F_W and u_t should both shift the saturation profile in the same direction, causing a monotonous saturation change at each position along the core, both for drainage and imbibition.

For a core of mixed wettability, F_W is increased and u_t is decreased when $p_c = p_o - p_w$ is positive (spontaneous imbibition) and F_W is further decreased but u_t should be increased again when p_c is negative (forced imbibition).
[We use the notation that the water saturation decreases during drainage and increases during imbibition, whether the core is waterwet or not.]

The interpreted results together with the input data for the waterwet case are shown to agree well in Figs. 7-9.

Conclusions

A new multirate steady-state method to determine relative permeability from core flooding experiments has been developed.

The experimental procedure consists of a number of conventional steady-state experiments with different fractional flow values and different total rates. It is necessary to design the experiment such that all parts of the core follow the same hysteresis curve, primary drainage or primary imbibition.

The method has been demonstrated by simulation experiments. Cases of water wet and mixed wet rocks, with and without hysteresis have been considered.

Acknowledgements

We thank Esso Norge for support and permission to publish the paper.

Nomenclature

A = cross sectional area of core
f = fractional flow function
F = fractional flow at the inlet end
k = absolute permeability
L = length of core
p = pressure
S = saturation
t = time
x = coordinate
u = velocity
ϕ = porosity
λ =mobility

Subscripts

c = capillary
cl = capillary limit
i = fluid phases or irreducible or inlet
o = oil
r = relative
t = total
vl = viscous limit
w = water

Superscripts

0 = @ $x = 0$
+ = inside the core @ $x = 0$
— = average
L = @ $x = L$

Operators

Δ = difference

References

1 Braun, E.M. and Holland, R.F.: "Relative Permeability Hysteresis: Laboratory Measurements and a Conceptual Model," paper SPE 28615 presented at the 1994 SPE Fall Meeting, New Orleans, Sept. 25-28.

2 Dale, M., Ekrann, S., Mykkeltveit, J., and Virnovsky, G.: "Effective Relative Permeabilities and Capillary Pressure for 1D Heterogeneous Media," presented at the 1994 European Conference on the Mathematics of Oil Recovery, Røros, June 7–10.

3 Eikje, E., Jakobsen, S.R., Lohne, A., and Skjaeveland, S.M.: "Relative Permeability Hysteresis in Micellar Flooding," *J. Pet. Sci. & Eng.*, 7 (1992) 91—103.

4 ECLIPSE 100, v. 95a, reference manual, Intera Information Technologies Limited, Highland Farm, Henley, Oxon, UK.

5 Killough, J.E.: "Reservoir Simulation With History-Dependent Saturation Functions," *SPEJ* (Feb. 1976) 37—48.

6 Longeron, D., Hammervold, W.L., and Skjaeveland, S.M.: "Water-Oil Capillary Pressure and Wettability Measurements Using Micropore Membrane Technique," paper presented at the 1994 International Symposium of the Society of Core Analysts, Stavanger, Sept. 12-14.

7 Marle, C.M.: *Multiphase Flow in Porous Media*, Gulf Publishing, Editions Technip, Paris, 1981.

8 Minssieux, L. and Duquerroix, J-P.: "WAG Flow Mechanisms in Presence of Residual Oil," paper SPE 28623 presented at the 1994 SPE Fall Meeting, New Orleans, Sept. 25-28.

9 Quandalle, P. and Sabathier, J.C.: "Typical Features of a Multipurpose Reservoir Simulator," *SPERE* (Nov. 1989) 475—80.

10 Ramakrishnan, T.S. and Capiello, A.: "A New Technique to Measure Static and Dynamic Properties of a Partially Saturated Porous Medium," *Chem. Eng. Sci.*, **46** No. 4, 1991, 1157–1163.

11 Richardson, J.G., Kerver, J.A., Hafford, J.A., and Osoba, J.S.: "Laboratory Determination of Relative Permeability," *Trans.* AIME, **195** (1952) 187–96.

12 Van Duijn, C.J. and de Neef, M.J.: "The Effect of Capillary Forces on Immiscible Two-Phase Flow in Strongly Heterogeneous Porous Media," paper presented at the 1994 European Conference on the Mathematics of Oil Recovery, Røros, June 7–10.

13 Virnovsky, G.A., Guo, Y., Vatne, K.O., Braun, E.M.: "Pseudo Steady State Technique for Relative Permeability Measurement". paper presented at the International Symp. of the SCA, Stavanger, Norway 1994, 217-226.

14 Virnovsky, G.A., Guo, Y., and Skjæveland S.M.: "Relative permeability and capillary pressure concurrently determined from steady-state flow experiments" paper presented at the 8th European Synp. on IOR, Vienna, Austria, May, 1995

15 Virnovsky, G.A., Guo, Y., Skjæveland S.M., Ingsoy, P. : "Steady state relative permeability measurements and interpretation with account for capillary effects" paper presented at the International Symp. of the SCA, San-Francisco, U.S.A., Sept., 1995

16 Yortsos, Y.C. and Chang, J.: "Capillary Effects in Steady-State Flow in Heterogeneous Cores," *Transport in Porous Media* **5**, 1990, 399—420.

Figures

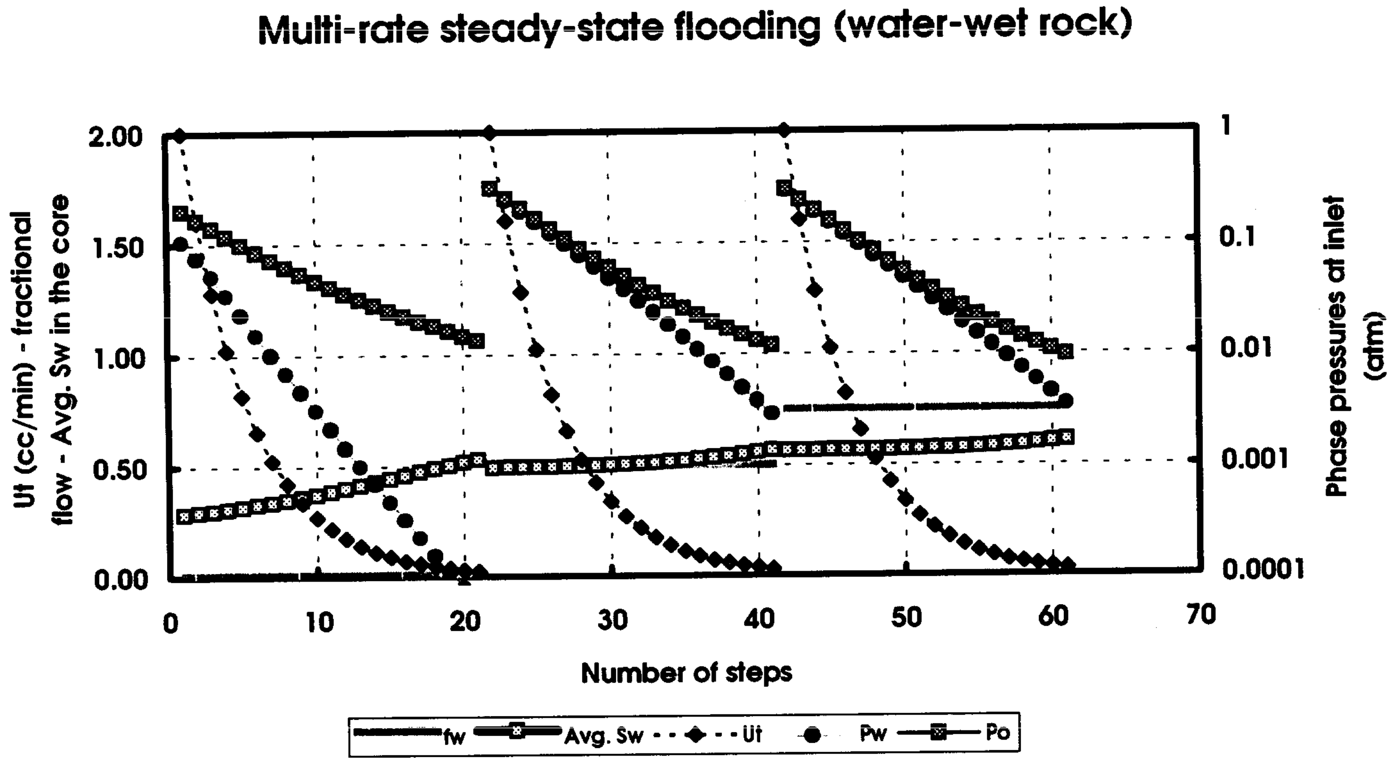

Figure 1 - Simulated responses from multirate, steady-state flooding, water-wet case.

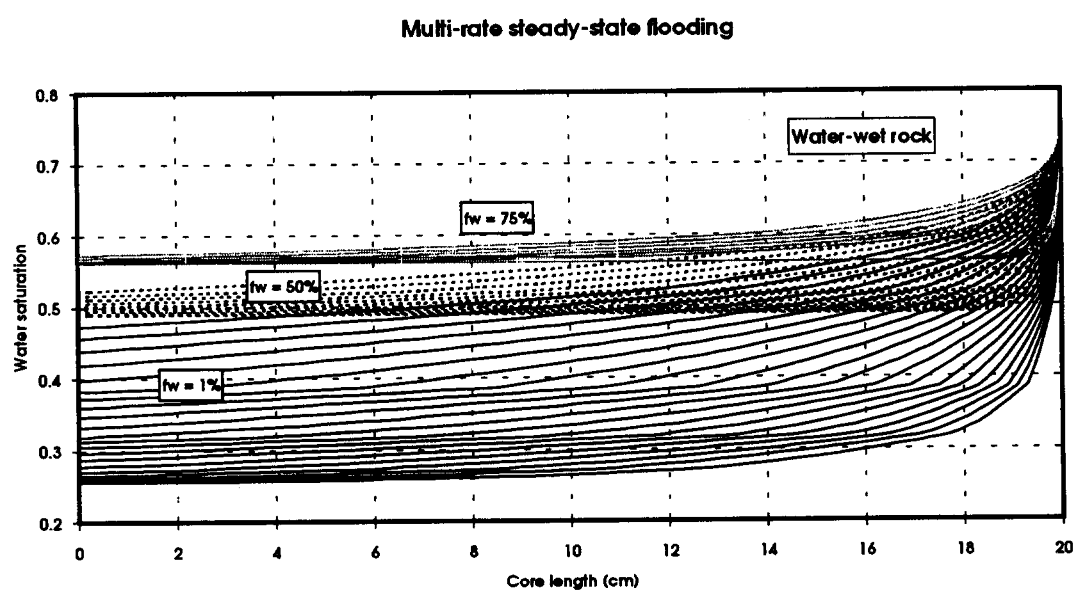

Figure 2 - Water saturation distribution from multirate, steady-state flooding, water-wet case.

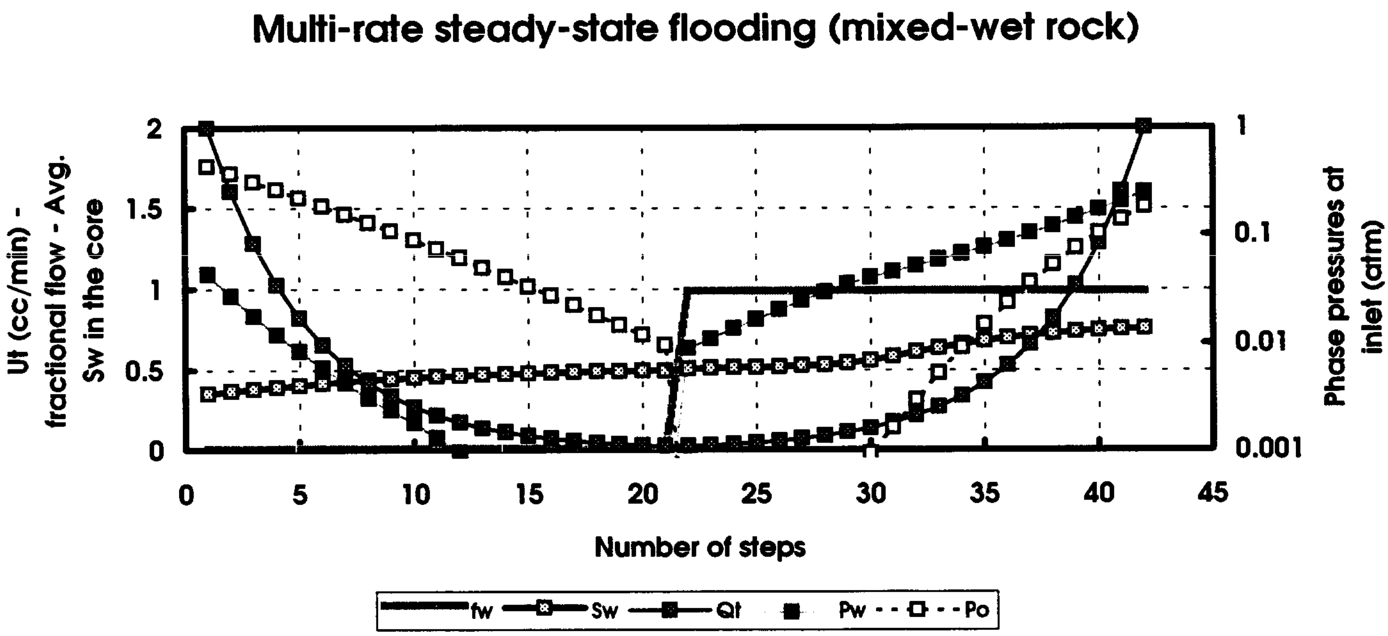

Figure 3 - Simulated responses from multirate, steady-state flooding, mixed-wet case.

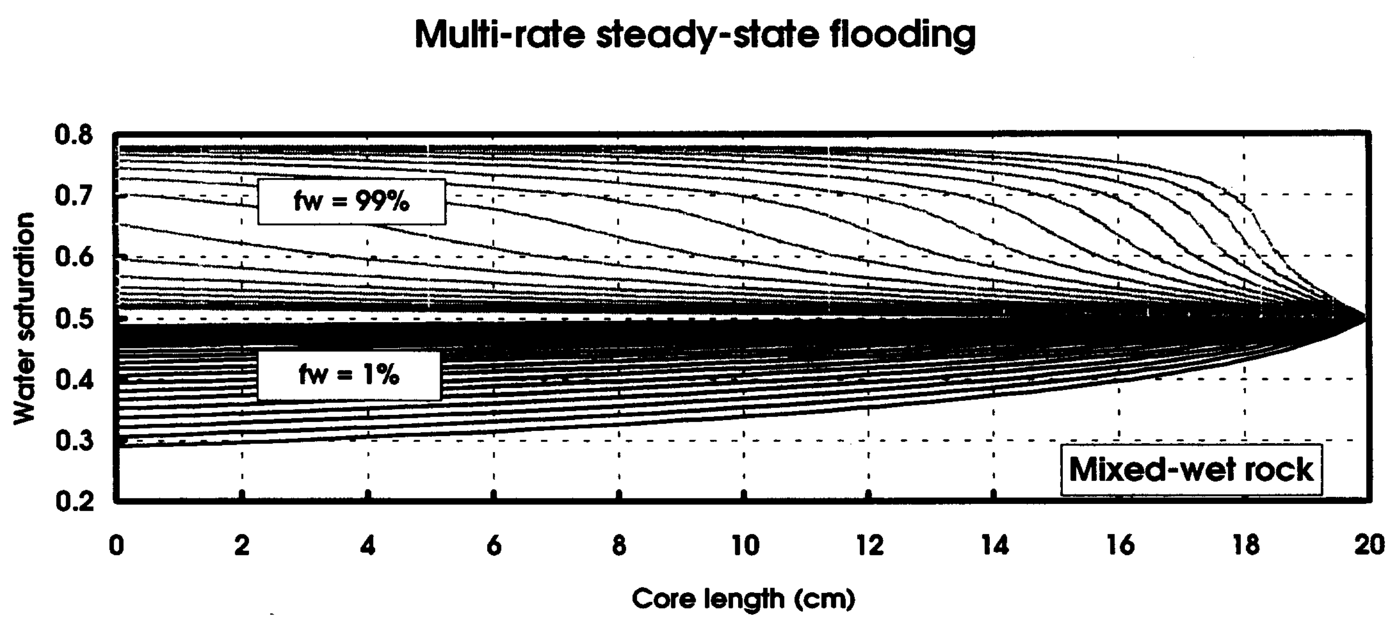

Figure 4 - Water saturation distribution from multirate, steady-state flooding, mixed-wet case.

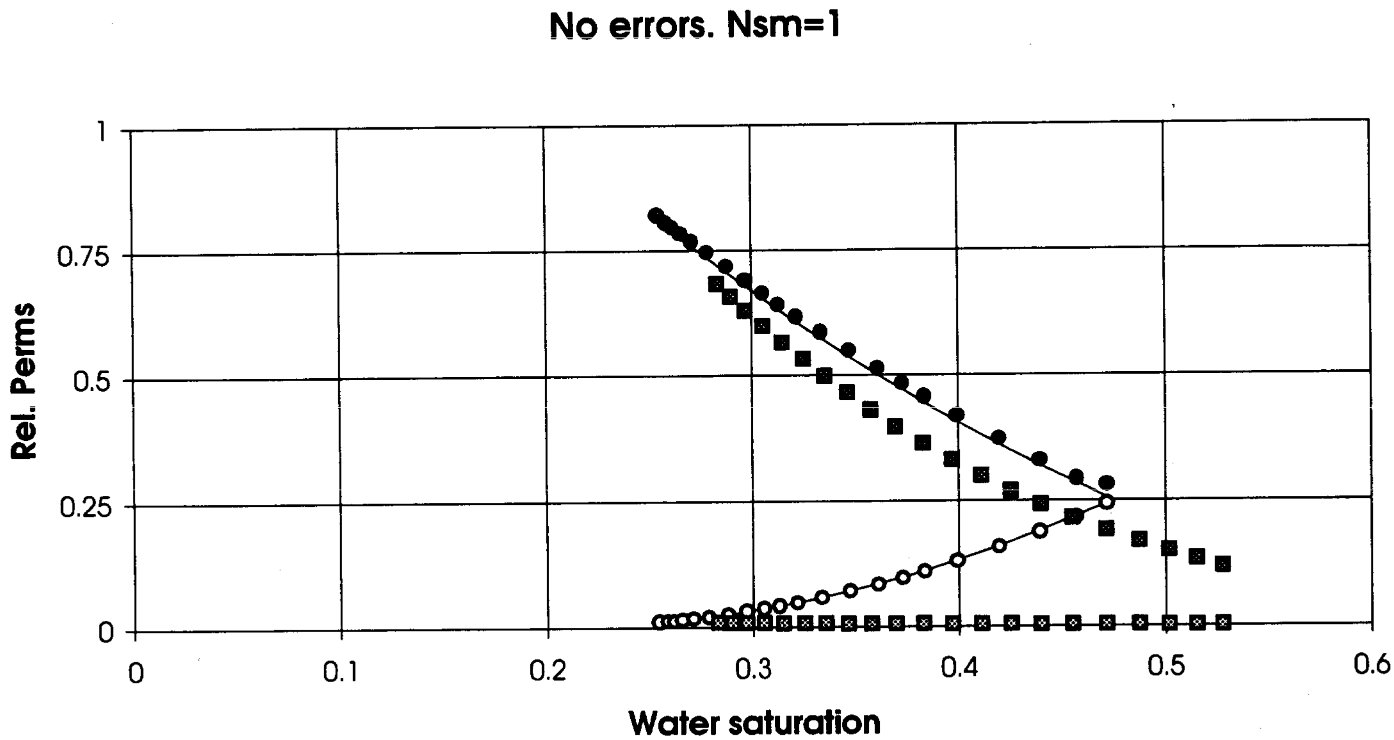

Figure 5 - Relative permeabilities from theory in this paper (circles); from Darcy's law with no corrections (squares); and true curves from input data (solid curves); water-wet case.

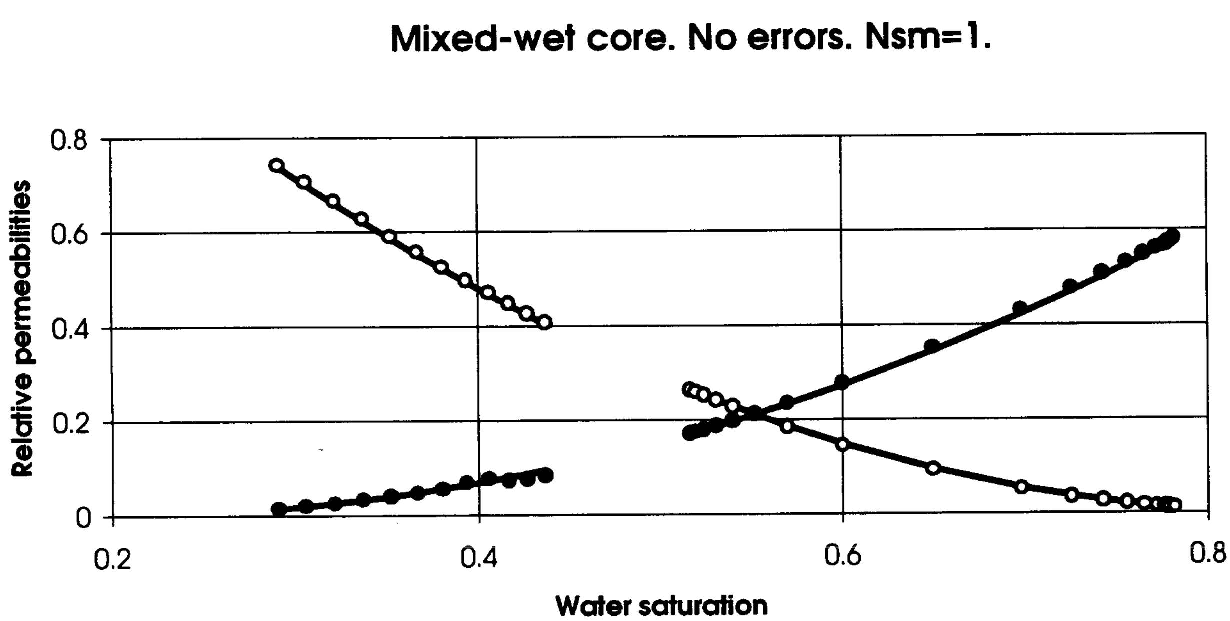

Figure 6 - Relative permeabilities; from theory in this paper (circles) and true values (solid curves) from simulator input.

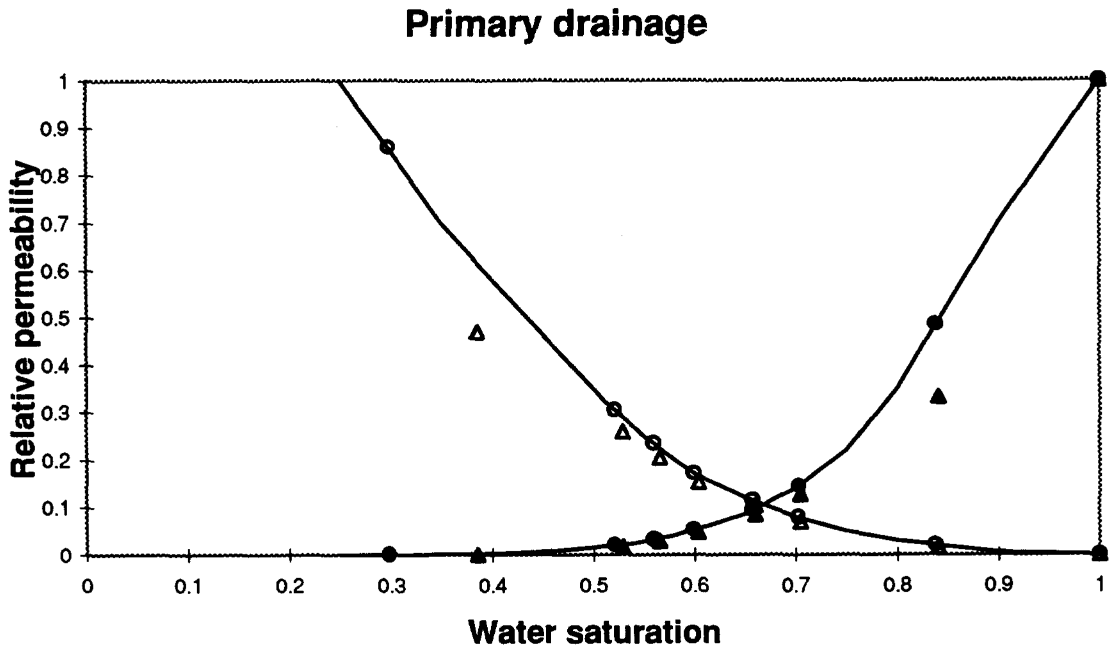

Figure 7 - Relative permeabilities determined at primary drainage conditions: from theory in this paper (circles); from Darcy's law with no corrections (triangles); and true curves from input data (solid curves); .

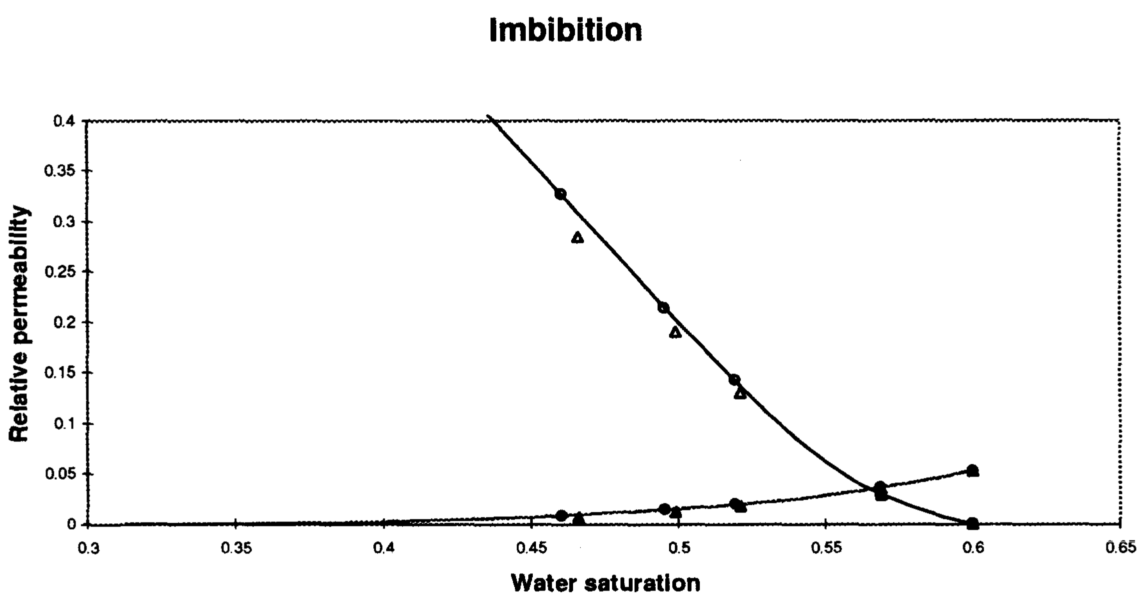

Figure 8 - Relative permeabilities determined at imbibition conditions: from theory in this paper (circles); from Darcy's law with no corrections (triangles); and true curves from input data (solid curves); .

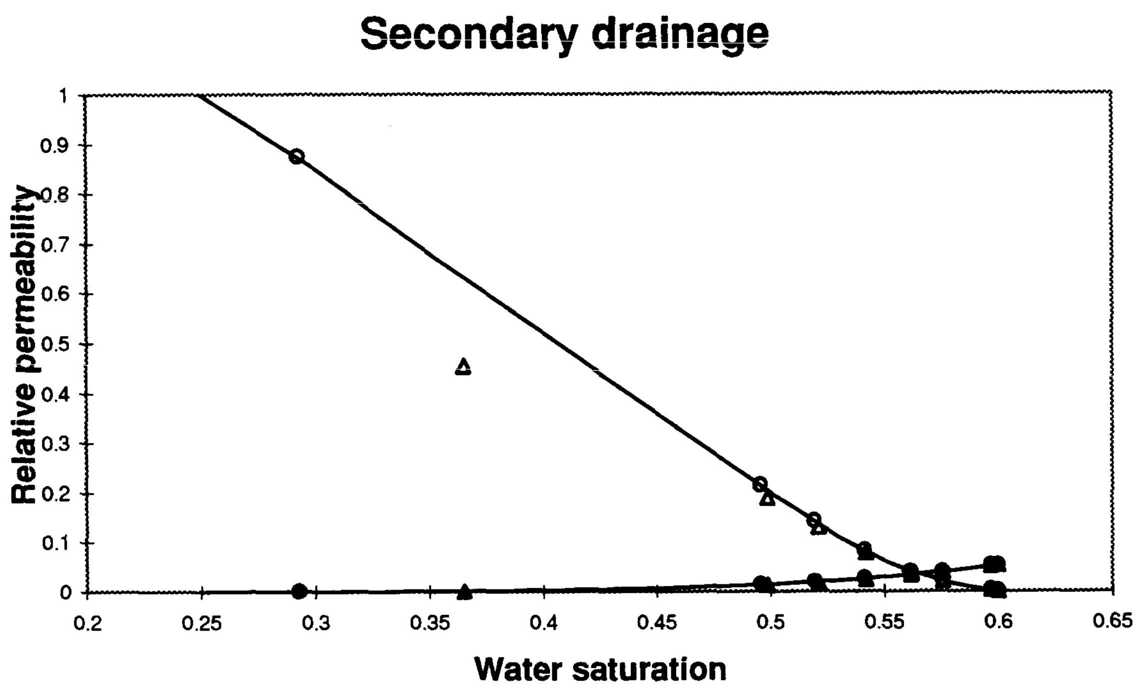

Figure 9 - Relative permeabilities determined at secondary drainage conditions: from theory in this paper (circles); from Darcy's law with no corrections (triangles); and true curves from input data (solid curves); .